SAND2017-6251C

COVER SHEET

Paper Number: **35**

Title: **Verification and Validation of Residual Stresses in Simple Composite Structures**

Authors: Stacy M. Nelson
Alexander A. Hanson
Timothy M. Briggs
Brian T. Werner

ABSTRACT

Process-induced residual stresses commonly occur in composite structures composed of dissimilar materials. These residual stresses form due to differences in the composite materials' coefficients of thermal expansion and the shrinkage upon cure exhibited by polymer matrix materials. Depending upon the specific geometric details of the composite structure and the materials' curing parameters, it is possible that these residual stresses could result in interlaminar delamination or fracture within the composite. Therefore, the consideration of potential residual stresses is important when designing composite parts and their manufacturing processes. However, the experimental determination of residual stresses in prototype parts can be time and cost prohibitive. As an alternative to physical measurement, it is possible for computational tools to be used to quantify potential residual stresses in composite prototype parts. Therefore, the objective of this study is the development of a simplistic method for simulating the residual stresses formed in polymer matrix composite structures. Specifically, a simplified approach accounting for both coefficient of thermal expansion mismatch and polymer shrinkage is implemented within the Sandia National Laboratories' developed SIERRA/SolidMechanics code Adagio. Concurrent with the model development, two simple, bi-material structures composed of a carbon fiber/epoxy composite and aluminum, a flat plate and a cylinder, are fabricated and the residual stresses are quantified through the measurement of deformation. Then, in the process of validating the developed modeling approach with the experimental residual stress data, manufacturing process simulations of the two simple structures are developed and undergo a formal verification and validation process, including a mesh convergence study, sensitivity analysis, and uncertainty quantification. The simulations' final results show adequate agreement with the experimental measurements, indicating the validity of a simple modeling approach, as well as a necessity for the inclusion of material parameter uncertainty in the final residual stress predictions.

Sandia National Laboratories, Livermore, CA 94541-0969

1. INTRODUCTION

Sandia National Laboratories is a multimission laboratory managed and operated by National Technology and Engineering Solutions of Sandia, LLC, a wholly owned subsidiary of Honeywell International, Inc., for the U.S. Department of Energy's National Nuclear Security Administration under contract DE-NA0003525.

Fiber-reinforced composite materials provide superior strength-to-weight and stiffness-to-weight ratios when compared to metals. However, when considering the utilization of composite materials, perhaps in place of a metal, certain material behaviors must be considered. One material phenomenon that is known to exist within composite parts and that can cause interlaminar delamination within a laminated composite, is the presence of manufacturing process induced residual stresses [1-2]. These residual stresses form during the elevated temperature curing cycles required of most composite material systems due to differences in the composite materials' coefficients of thermal expansion, as well as the shrinkage upon cure exhibited by thermoset polymer matrix materials. While experimental methods can be used to quantify the post manufacturing stress state of a composite component, an experimental approach becomes less practical as the composite structure under examination becomes complex. As an alternative, validated computer simulations, which model the composite materials' elevated temperature cure cycles, can instead be used to predict the post-fabrication stress state. This approach represents not only a cost and time savings when compared to physical experimentation, but it also presents the ability to understand the residual stress state in any structure, regardless of complexity.

In order for representative predictions of a post-fabrication stress state to be made, finite element methods must be developed which sufficiently account for the physical changes undergone by a composite during its curing process. Upon review of the existing literature, two primary methods for simulating these changes were observed. The first method documented is complex, as it simulates the complete evolution of the composite material's mechanical properties functionally dependent upon the cure state. Specifically, both White, et. al., and Tavakol, et. al., present highly detailed modeling methodologies and constitutive models, which incorporate most of the physics relevant to the polymer curing process [3-5]. Alternatively, the second method is much simpler, as the totality of a composite's fabrication processing details are accounted for through the experimental determination of the stress-free temperature, which is related to the temperature at which the polymerization reaction occurs. As discussed by both Jumbo, et. al., and Hanson, et. al., it can safely be assumed that a composite's final residual stress state depends only upon the composite's materials' coefficients of thermal expansion and thermal excursions from the stress-free temperature [6-7]. Interestingly, regardless of the modeling method's fidelity, the predictions associated with both the complex and simple finite element approaches discussed in literature were well validated experimentally.

1.1 Objectives

Examples from literature have indicated that accurate predictions of a composite's post-fabrication stress state can be made with a simple approach, dependent only upon the stress-free temperature. Therefore, the objectives of this study are related to the development of a simple and robust methodology for the simulation of process-induced residual stresses within composite structures. A method based upon the work of Jumbo, et. al., will be developed and implemented within Sandia National Laboratories developed SIERRA/SolidMechanics code. The developed finite element methods will account for the formation of stresses within

rigid composite structures immediately following their birth during the polymerization reaction at elevated temperatures. As these residual stresses are primarily due to the materials' dissimilar coefficients of thermal expansion, the modeling methodology will take advantage of material models capable of accurately simulating thermal strains. Concurrent with these modeling efforts, experiments will be completed to quantify the residual stresses formed in a simple composite part. Specifically, open-ended cylinders will be designed and manufactured from two dissimilar materials, carbon fiber/epoxy composite and aluminum, such that measurable residual stresses will be present. Upon completion of these residual stress experiments, the developed simulation methods will be applied to approximate the cylinders' manufacturing process for model validation. However, since it is anticipated that there will be some uncertainty in the constitutive model parameters required during the finite element process, a formal sensitivity study will be completed to understand which of those model parameters are most influential to the residual stress state predictions, and then the uncertainty in those critical parameters can be characterized and propagated through the process model to form a prediction based upon the expected material irregularities.

2. EXPERIMENTAL METHODS

A significant experimental effort was conducted concurrently with the model development to provide material parameters and data for model validation. Specifically, a flat plate and an open-ended cylinder were designed and manufactured from composite and metallic materials. Then, after the parts were manufactured, the flat plate was tested to determine the composite's stress-free temperature and the open-ended cylinder was used to demonstrate residual stresses developed as measurable deformations.

2.1 Plate and Cylinder Materials and Manufacturing

The flat plate and open-ended cylinder were both composed of a carbon fiber/epoxy composite material and an aluminum alloy. The carbon composite consisted of AS4C tows in an 8-harness satin weave pattern, which were preimpregnated with a TCR 3362 resin. Prior to the manufacturing of the simple composite parts, the exterior surfaces of a flat aluminum plate and a thin-walled aluminum cylinder were lightly abraded and cleaned with acetone in preparation for bonding with the carbon composite. Then, flat, uncured laminates of the composite material were either placed on top of the prepared aluminum plate or wrapped around the prepared aluminum cylinder. Lastly, the uncured composite parts underwent a standard vacuum bagging process within an autoclave with an applied temperature and pressure of 177°C and 0.31 MPa, respectively,

The composite plate was specifically composed of an aluminum 6061-T6 plate, which measured 457.20 mm by 457.20 mm by 0.81 mm, with a centered 406.4 mm square laminate of the carbon composite. Alternatively, the cylinder was composed of an aluminum 6063-T6 inner cylindrical liner, which had an outer diameter of 112.30 mm and wall thickness of 2.03 mm, with a laminate of the carbon composite overwrapping the aluminum liner's exterior surface. Note that for both the plate and

cylinder, the composite laminate consisted of four plies of the 8-harness satin weave fabric with a stacking sequence of $[0_2]_s$.

2.2 Residual Stress Measurement Procedure and Results

2.2.1 DETERMINATION OF THE STRESS FREE TEMPERATURE

As shown by the literature, with a simplistic modeling approach, the material property most important to accurate predictions of the final residual stress state is the stress-free temperature. Therefore, the composite plate, was placed in a furnace at ambient temperatures and heated progressively to a final temperature of 160ºC (figure 1). Evident from the top left image in the figure below, immediately following manufacturing, residual stresses within the composite plate caused distortion with curvature along the plate's main diagonal. Therefore, at regular intervals throughout the heating of the plate, the temperature of the furnace was programmed to dwell such that the "flatness" of the plate could be observed. This process is shown below in figure 1. The stress free temperature of the plate appears to be between 140.6ºC and 146.1ºC, as the plate appears the flattest between these two observations. Therefore, the final stress-free temperature of the plate was specified as 143.3°C, or the average of the two probed temperatures, and this value was used in the finite element simulations.

2.2.2 RESIDUAL STRESS MEASUREMENT IN A COMPOSITE CYLINDER

The manufactured open-ended cylinder was designed to exhibit significant residual stresses visually through physical deformation. However, as the cylinder represents a stable configuration, residual stresses were not obviously exhibited post-manufacturing. Therefore, in order to permit a measurable deformation, the cylinder was sectioned into multiple 25.4 mm wide rings and then a 35°, or 32.5 mm wide, circumferential sector was removed from each of the sectioned rings. This process of removing the sectors created a gap in each of the rings which would close in on itself due to the residual stresses present at the bi-material interface. Figure 2 describes the ring's preparation for residual stress measurement.

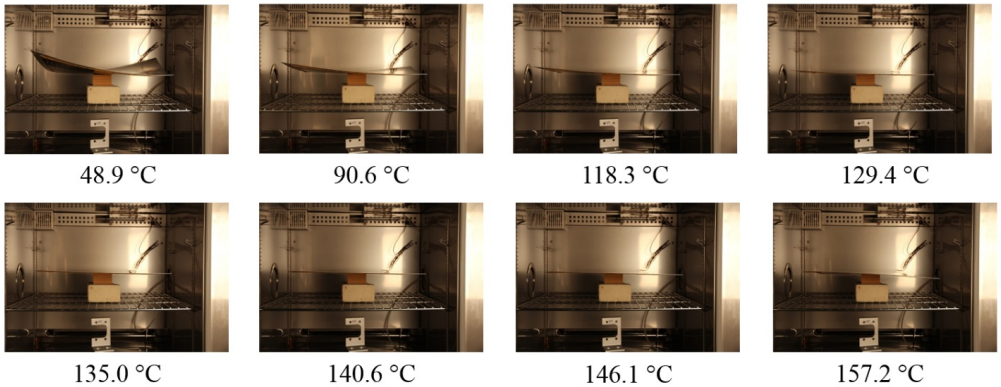

Figure 1: Composite plate distortions at various temperatures

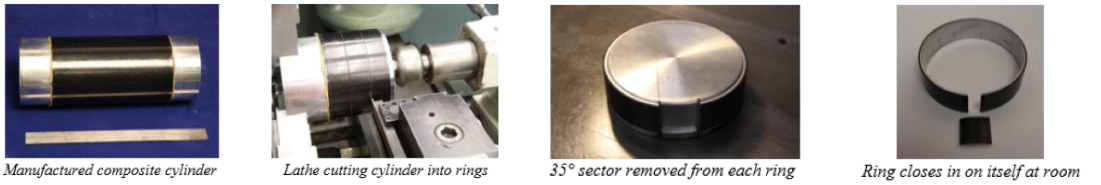

Figure 2: Preparation of the composite cylinder for residual stress measurement

After the composite rings were removed from the cylinder and split through the sector removal process, each specimen was placed in a furnace and subjected to two thermal cycles, heating from 25°C to 160ºC and cooling from 25°C to -50ºC. During this temperature cycle, the width of the gap left in each of the rings by the removed sector was monitored with a clip-on static extensometer. Figure 3 shows the representative gap change recorded by the extensometer.

3. FINITE ELEMENT ANALYSIS

Concurrent with the experiments, modeling methods were developed to accurately predict the residual stresses formed in composite parts during the fabrication process. These developed modeling methods were then used to simulate the manufacturing of the split rings discussed in the preceding section for validation.

3.1 Methods

3.1.1 ANALYSIS SOFTWARE

All of the completed simulations utilized Sandia National Laboratories' SIERRA/ SolidMechanics code, Adagio. Adagio is a Lagrangian, three-dimensional code for the finite element analysis of solid structures and is suitable for implicit, quasi-static analyses, such as the manufacturing process simulations of the composite rings.

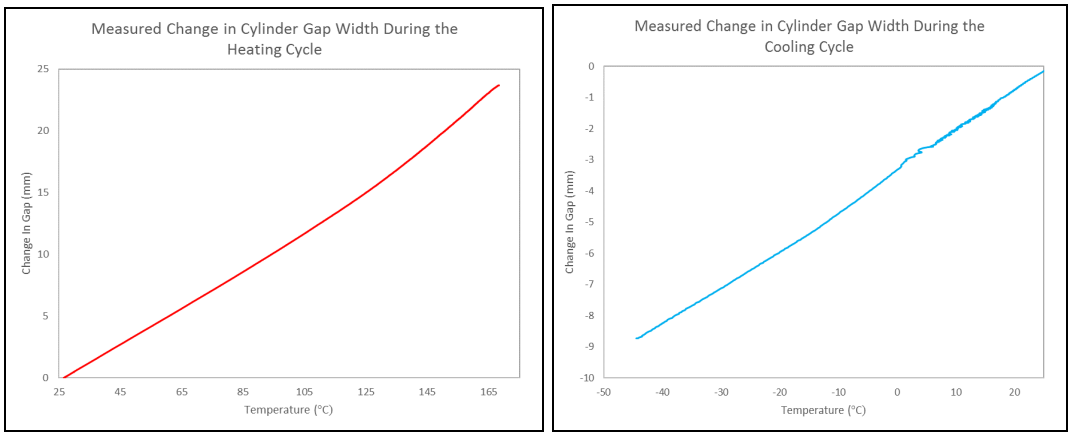

Figure 3: Measured change in cylinder gap width for the heating (left) and cooling (right) cycles

Adagio makes use of a multi-level solver, of which the solution core is a nonlinear, conjugate gradient algorithm that can iteratively find a solution that is within some user-defined tolerance of equilibrium. Use of the multi-level solver assists in the solution of problems, like the split composite ring, which models materials with non-linear responses or extreme differences in stiffness. [8].

3.1.2 ELEMENT FORMULATION

The three dimensional cylinder models were simulated with eight-noded hexahedral elements. For efficiency, the element formulation default to Adagio was used. This formulation conducts the volume integration with single point Gaussian quadrature and, although it is computationally inexpensive, it exhibits zero energy, or "hourglassing," modes. However, a simple method of controlling this undesirable behavior is the application of a small elastic stiffness that is capable of stopping the formation of any anomalous modes without affecting the global response. Sierra Adagio is automatically equipped with a default "hourglassing" stiffness of 0.05 and this value was used in all of the completed analyses. [8]

3.1.3 MATERIAL MODELS

The manufacturing process models of the simple composite structures required the definition of three separate materials, the uncured carbon/epoxy composite, the cured carbon/epoxy composite, and the aluminum alloy, and these three materials were defined in simulation with just two materials models.

Firstly, as no plastic deformation was expected for the aluminum liner, it was modeled with Sierra Adagio's elastic material model. This model describes a simple linear-elastic behavior and the only material properties required for its use are: a thermal strain function related to the material's coefficient of thermal expansion, Young's modulus, and Poisson's ratio [8]. Table I summarizes the material properties used to define the elastic material model for both the aluminum 6061 and 6063 alloys [9].

Secondly, in the uncured state, the composite's epoxy matrix material has the ability to flow and its response is dominated by the adjacent aluminum components, which behave isotropically. Therefore, the uncured carbon composite was modeled as a compliant and incompressible, isotropic-elastic solid with that same elastic material model used to define the response of the aluminum. Table II summarizes the properties defining the uncured composite material.

Table I: Elastic material properties of the aluminum alloys

Density (kg/m^3)	2,700	**Poisson's Ratio**	0.33
Young's Modulus (GPa)	68.9	**CTE (1/ºC)**	23.4e-06

Table II: Elastic material properties of the uncured composite material

Density (kg/m^3)	1,600	**Poisson's Ratio**	0.499
Young's Modulus (GPa)	0.1	**CTE (1/ºC)**	23.4e-06

Table III: Elastic orthotropic material properties for the cured composite material

Density (kg/m^3)	1,600	
E_{11}, E_{22}, E_{33} (GPa)	63.86, 62.74, 8.59	
ν_{12}, ν_{13}, ν_{23}	0.0480, 0.4075, 0.0548	
G_{12}, G_{13}, G_{23} (GPa)	3.44, 3.27, 3.25	
T_g (°C)	125.1	
T_{sf} (°C)	143.3	
	Glassy Region	**Rubbery Region**
CTE_{11} (1/°C)	3.40e-06	1.13e-06
CTE_{22} (1/°C)	3.36e-06	1.13e-06
CTE_{33} (1/°C)	7.20e-05	2.83e-04

Lastly, the cured carbon composite material was defined with Adagio's elastic orthotropic material model, which simulates linear-elastic, orthotropic material behaviors. The model's parameters, which are related to the composite's elastic and thermal behaviors, were determined with either standardized mechanical tension tests, micromechanical representative volume models, or thermomechanical analysis experiments and are summarized in table III.

3.1.4 MODEL GEOMETRY AND APPLIED BOUNDARY CONDITIONS

A three dimensional geometry and discretized mesh was created for the split composite rings (figure 4) using Cubit, which is a robust software toolkit capable of creating both two- and three-dimensional geometries and meshes. In the developed model, the aluminum and composite materials were modeled as separate, homogenized material layers with the dimensions specified in the previous section. Also, the split ring model assumed symmetry along two planes for computational efficiency. As shown in figure 4, symmetry conditions were assumed across both the 12- and 13-planes. Also, the ring was simulated as a net shape, instead of as part of a larger cylinder (as shown by the manufacturing process in figure 2). It was assumed that since the aluminum underwent no plastic deformation during the composite curing process, the rings could be modeled in their final configuration, as the stresses developed in a net shaped ring were expected to be only negligibly different from the stresses formed over a similar volume as part of a larger cylinder.

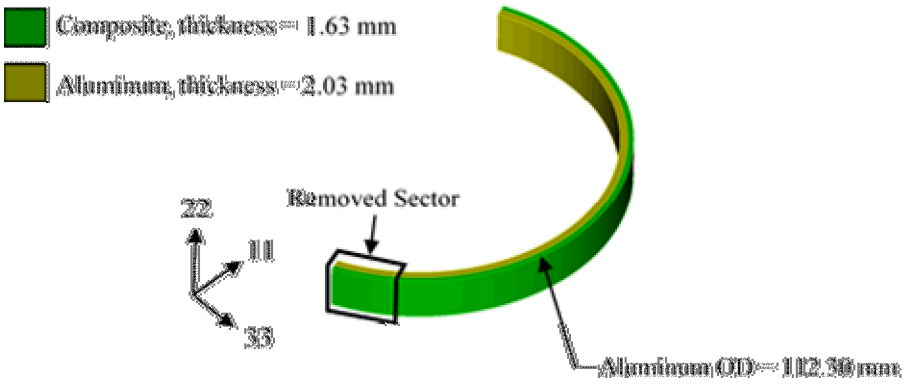

Figure 4: Composite ring simulation geometry

In addition to symmetry conditions, boundary conditions were applied to simulate the composite ring's heating and cooling, as well as the sector removal for residual stress relief. Specifically, the complete simulation of the composite ring's curing, sector removal, and subsequent re-heating and cooling took place in three steps. In the first step, temperature boundary conditions were applied to simulate heating and cooling from ambient conditions to the stress-free temperature (143.3°C). Then, the hexahedral elements of the ring model labeled "removed sector" (figure 4) were omitted from the simulation and the stresses along the newly freed edges were allowed to relax. Lastly, the split ring was subjected to an additional thermal cycle to simulate the experiment's heating to 160ºC and the cooling to -50ºC. Details regarding the simulation of the composite's curing process and sector removal are provided in the following section.

3.1.5 ELEMENT ACTIVATION AND DEACTIVATION

The manufacturing process model of the split composite ring simulates two processes: the matrix material's stiffness change during the polymerization reaction and the removal of material due to a machining process. These two processes were approximated within Sierra Adagio with element "activation" and "deactivation," and the transferring of stress, strain, and displacement states between subsequent simulations. With these techniques, an initial simulation can be completed in which one or more component representing the uncured composite is modeled with very compliant material properties until a temperature indicative of the polymer's curing conditions is reached. Any component in this initial simulation modeled with the compliant properties will deform according to the non-compliant components without affecting the behavior of the stiffer parts. Once the curing temperature is reached, the simulation can be ended and stress, strain, and displacement data can be saved to an output file. Then, a new simulation can be performed in which the input geometry, displacements, and states of stress and strain are transferred from the output of the previous simulation. At the onset of this second simulation, the material parameters of the initially compliant parts can be set to their actual values, "activating" the previously compliant components and simulating the stiffness change undergone by a curing polymer. Furthermore, to mimic a machining process to remove material after the initial curing step, Sierra permits the omission, or "deactivation," of any unwanted model components with the "omit" command. Specifically, the "omit" command can be used to remove any unwanted model component at the onset of a new simulation. When an omission in employed, the deactivated component is removed from the model and all stress, strain, and displacement data associated with the omitted parts are permanently deleted.

The element activation and deactivation process was applied to approximate the composite ring's manufacturing in four simulations. In the first simulation, the ring was virtually heated from ambient conditions to the stress-free temperature with the uncured composite's behavior defined with the properties given in table II. Then, once the stress-free temperature was reached, this initial simulation ended and the ring's stress, strain, and displacement states were written to an output file. Then, a second simulation was initiated, with the input transferred from the previous simulation's output file. The boundary conditions applied in this second simulation virtually cooled the composite ring from the stress-free temperature back to the

ambient conditions with the composite's behavior switching from compliant to stiff. A third simulation was then initiated in which the "removed sector" section of the ring geometry was "deactivated" and the model was allowed to reach stress equilibrium. Finally, in a fourth simulation, the split ring was subjected to a realistic thermal cycle (-50 ºC to 160ºC) and the sector's gap width was monitored.

3.2 Mesh Convergence Study

A grid convergence study was completed prior to undertaking the uncertainty quantification to verify the analysis methods described in the preceding sections, as well as to determine the maximum permissible element size for a confident prediction. Specifically, the discretization errors associated with the process-induced residual stresses within the split ring were determined with a Richardson's Extrapolation based mesh convergence study. This method allows for the approximation of a higher order estimate of a continuum solution given a series of three, lower order, discrete solutions [10-11]. These low order solutions were determined through the discretization and simulation of the model shown in figure 4 with three uniformly refined mesh sizes, 0.8143 mm, 0.4071 mm, and 0.2036 mm, and the finite element methods discussed in the preceding sections.

The metric upon which mesh convergence was measured was the gap width remaining from the removed sector at ambient conditions. Therefore, with the gap width predictions resulting from the three uniformly refined models, the Richardson's extrapolated exact solution was found to be 12.36 mm. Figure 5 shows both the relationships between the simulated solutions and the discretization errors with mesh size. As shown in this plot, the discretization errors decrease with each level of mesh refinement, indicating that the discrete solution simulations are converging to the extrapolated exact value and this lends confidence to the modeling procedure. Furthermore, regarding the ideal mesh size for future simulations, all of the examined element sizes provided discretization errors less than 10% and both the coarsest and medium mesh levels provided reasonable solution times. Therefore, for computational efficiency, all remaining models were completed with the medium element size, which was 0.4071 mm.

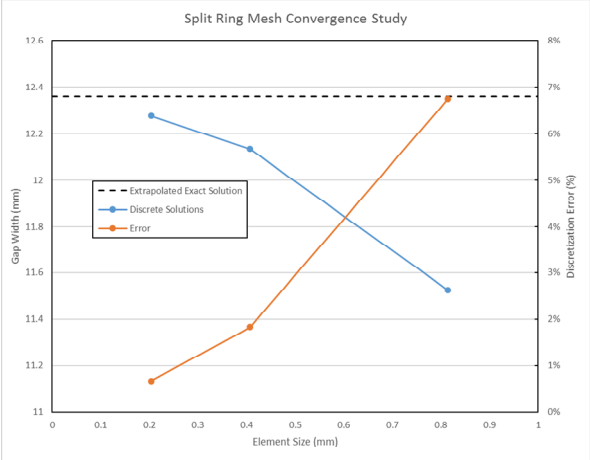

Figure 5: Richardson's extrapolation for the split ring

3.3 Input Parameter Sensitivity Analysis

While the mesh convergence study lends confidence to the modeling procedure, the material parameters defining the carbon composite were determined inexactly, with a combination of experiments and micromechanical modeling. Since the material characterization was not completed with consistency, uncertainties exist in the material properties that should be propagated through the finite element simulations to understand the effect of property variation on the residual stress predictions.

As shown in tables I and III, the composite ring's behavior is governed by 21 material property values. Ideally, the uncertainty in all of these parameters would be determined and propagated through the finite element models during a formal uncertainty quantification (UQ). However, the characterization of this number of parameters is both time and cost prohibitive. Therefore, prior to the quantification of the model's uncertainties, a formal sensitivity study was completed to determine which of the 21 model input parameters were truly influential to the simulated residual stress response. Then, only those critical parameters would be characterized and considered during the formal UQ process.

3.3.1 SENSITIVITY ANALYSIS METHODS

In initializing the sensitivity analysis, the 21 material parameters defined in tables I and III were used to develop a 21-dimensional parameter space. This parameter space was then sampled numerous times and each sampled parameter set was applied to simulate the split ring's manufacturing process. The technique selected to sample the parameter space was representative and organized, such that a minimum number of sample sets could be used to develop trends among the 21 individual input parameters and the simulated residual stress output. There are many different approaches that can be taken to efficiently sample a high dimensional parameter space. One such approach is the Box Behnken Design method (BBD). This approach, which was selected for the current sensitivity analysis, is highly stable, as it does not sample outside of the defined process, or parameter, space. In addition to improved stability, when compared to other sampling approaches, the Box Behnken method also seems to require fewer overall samples to develop trends between the input parameters and the output. The relationship between the number of computer experiments designed with the BBD approach and k potential input parameters can be expressed as $N=2k(k-1)$, where N is the number of experiments, or simulations, designed and k is the number of parameters [12]. Then, upon completion of the N simulations, the individual parameter sensitivities can be assessed with a multi-way analysis of variance (ANOVA). Specifically, the ANOVA represents a model independent, probabilistic sensitivity analysis method that can be used to determine the existence of statistical associations between an output response and one or more input parameters [13].

3.3.2 SENSITIVITY ANALYSIS RESULTS

With the methods described in the preceding section, a Box-Behnken sensitivity analysis was completed for the composite split ring. The study specifically

examined the influence of the 21 model parameters on the fabrication induced residual stresses predicted through simulation. As mentioned, the BBD methodology was used to sample the 21-dimensional parameter space. Therefore, as a first step, engineering judgement was used to define plausible minimum and maximum values for each of the parameters of interest, such that the parameter space could be bounded by realistic minimum and maximum values. These parameter ranges are described in table IV. With these ranges, the BBD method was used to develop a 21-dimensional parameter space and design 841 individual simulations. Upon completion of these simulations, the results were assessed, and the same residual stress metric upon which mesh convergence was measured (refer to section 3.2) was compared for the 841 predictions with a multi-way ANOVA. Upon completion of the ANOVA, main effects plots were created to assess each of the potentially influential parameters and table V summarizes the parameters found to be critical.

Table IV: Parameter ranges sampled by BBD

	Parameter	**Minimum Value**	**Maximum Value**
Composite Properties	E_{11} (GPa)	57.5	70.2
	E_{22} (GPa)	56.5	69.0
	E_{33} (GPa)	7.7	9.4
	ν_{12}	0.043	0.053
	ν_{13}	0.367	0.449
	ν_{23}	0.367	0.448
	G_{12} (GPa)	3.1	3.8
	G_{13} (GPa)	2.9	3.6
	G_{23} (GPa)	2.9	3.6
	T_g (ºC)	110.9	141.8
	T_{sf} (ºC)	140.6	146.1
	CTE_{11} (1/ºC, rubbery)	0.294e-6	1.913e-6
	CTE_{22} (1/ºC, rubbery)	0.357e-6	2.794e-6
	CTE_{33} (1/ºC, rubbery)	268.1e-6	290.9e-6
	CTE_{11} (1/ºC, glassy)	3.060e-6	3.708e-6
	CTE_{22} (1/ºC, glassy)	2.585e-6	4.165e-6
	CTE_{33} (1/ºC, glassy)	67.8e-6	76.5e-6
	Thickness (mm)	3.40	3.55
Aluminum Properties	E (GPa)	57.0	85.6
	ν	0.264	0.396
	CTE (1/ºC)	18.7e-6	28.1e-6

Table V: Summary of the split ring's critical model parameters

	Critical Model Parameters
Composite Properties	E_{11}
	ν_{12}
	T_g
	T_{sf}
	CTE_{11} (rubbery)
	CTE_{11} (glassy)
	CTE_{33} (rubbery)
	CTE_{33} (glassy)
	Thickness
Aluminum Properties	E
	ν
	CTE

According to table V, 12 of the original 21 parameters are critical for predictions of the split ring's residual stress state. These 12 critical parameters seem intuitively correct. Particularly, as the aluminum alloy's response dominates during the initial portion of the structure's fabrication process, the metal's elastic and thermal properties should be influential to the final residual stress state. The remaining critical parameters are related to the composite's in-plane (12) elastic response, as well as the material's thermal behavior. These parameters are also intuitively acceptable, as the composite's rate of thermal expansion in the different orthotropic directions and its resistance to the deformation of the dominating aluminum substrate would significantly affect the split ring's final state of stress.

3.4 Uncertainty Quantification

The sensitivity analysis was completed to determine which material model input parameters must be included during the uncertainty quantification of the composite ring's simulated manufacturing process. The outcome of this study has indicated that only some of the parameters defining the composite's behaviors truly influence the residual stress predictions. Therefore, a significant effort was undertaken to characterize the expected material variations in those critical model parameters. Then, those variations were propagated through the process simulations to form residual stress prediction with the inclusion of realistic material parameter uncertainties.

3.4.1 UNCERTAINTY QUANTIFICATION METHODS

Upon completion of a sensitivity analysis, significant effort should be expended in the process of exactly characterizing those parameters found to be critical. However, generally, it is possible that certain critical material parameters cannot be determined experimentally. Nonetheless, it is likely that through additional numerical analyses or thorough literature surveys, accurate ranges in which the critical parameters may fall can be determined. Then, given distributions that describe the influential input parameters, uncertainty quantification can be used to propagate input parameter uncertainties though a simulation to determine the corresponding uncertainty in the predicted output response. This is readily achieved by sampling each input parameter range n times, creating n sets of sampled parameters. Then, n simulations can be processed in which the material model is defined with the n parameter sets. The resulting distribution of n simulation responses will represent the output range corresponding to the input parameter uncertainties [14].

The statistical method used to create the n parameter sets sampled from the input ranges is important, as full coverage of the parameter space needs to be guaranteed. A sampling method that is commonly used to construct computer experiments is the Latin Hypercube Sampling (LHS) approach. Given a predefined number of sample points, the LHS method can be used to ensure that a random ensemble of sampled variables is truly representative of reality [15]. Therefore, this approach was chosen for the ensuing uncertainty quantification study.

3.4.2 UNCERTAINTY QUANTIFICATION RESULTS

As discussed in the preceding sections, 12 model parameters were specified as critical for the split ring manufacturing process model. Of these 12 parameters, the uncertainties associated with 9 were determined experimentally. Specifically, the uncertainties associated with E_{11} and ν_{12} were determined with in-plane, mechanical tension tests as the standard deviations resulting from the repeated measurements. Similarly, uncertainties in the coefficients of thermal expansion and the T_g were also defined by the standard deviations resulting from repeated thermomechanical analysis experiments. Likewise, uncertainty in the composite's thickness was specified as the standard deviation resulting from several repeated radial measurements of the split ring's thickness. Alternatively, however, the variation in the T_{sf} was determined from the pre-existing data from the composite plate experiment discussed in section 2.3. Since this represents a single experiment, a range of potential T_{sf} values can be determined, but there can be no confidence in a numerical deviation.

The experimentally determined parameter uncertainty ranges are provided in table VI. Note that, with the exception of the T_{sf}, all of the parameters listed in this can be represented by a mean value plus-or-minus some deviation. Therefore, the corresponding uncertainty ranges for these 8 parameters can be characterized by normal distributions. However, since the experimental determination of the T_{sf} was made with only one experiment, its associated uncertainty is characterized as a uniform distribution, since probability data does not exist to weigh one portion of the experimental temperature range over another.

The three remaining critical parameters were specified within plausible ranges with a review of literature. As with the T_{sf}, the plausible material property variations found for these three parameters could not be weighed with respect to a known distribution and were, therefore, characterized as uniform distributions. Table VII defines these material property ranges defined through the review of literature.

Table VI: Critical material parameter variations determined through testing

Critical Model Parameters	**Uncertainty Range**	**Distribution Type**
E_{11} (GPa)	63.9 ± 2.4	Normal
ν_{12}	0.048 ± 0.019	Normal
T_g (°C)	125.1 ± 7.2	Normal
T_{sf} (°C)	285→295	Uniform
CTE_{11} (rubbery) (1/ºC)	1.127e-6 ± 0.582e-6	Normal
CTE_{11} (glassy) (1/ºC)	3.399e -6 ± 0.207e-6	Normal
CTE_{33} (rubbery) (1/ºC)	282.8e-6 ± 5.983e-6	Normal
CTE_{33} (glassy) (1/ºC)	71.990e-6 ± 2.379e-6	Normal
Thickness (mm)	3.496 ± 0.047	Normal

Table VII: Critical material parameter variations determined through literature review

Critical Model Parameters	**Uncertainty Range**	**Distribution Type**
E (GPa)	68.2→69.6	Uniform
ν	0.327→0.333	Uniform
CTE (1/ºC)	22.2e-6→24.6e-6	Uniform

With the normal and uniform distributions representing the 12 critical parameters, a formal uncertainty quantification process was completed to understand the effect of input parameter variations on the residual stress predictions. Specifically, with the methods described in the previous section, the LHS method was used to sample the ranges of values specified in the above tables 100 times, creating 100 sets of sampled parameters. These 100 parameter sets were then applied to the material models in 100 simulations and these simulations were processed within Sierra Adagio. Upon completion, a distribution of the same residual stress metric upon which mesh convergence was measured (section 3.2) were generated and checked for either normality or uniformity with a probability-probability (p-p) plot, which is a simple method to determine how well a set of data follows a particular distribution [13]. In creating a p-p plot, empirical data resulting from computer simulations are plotted versus the inverse of the theoretical cumulative distribution function of the distribution of interest and, if the resulting plot is approximately linear, the empirical, or simulated, data presents a good fit to the theoretical distribution. Figure 6 shows the p-p plot resulting for the split ring's UQ simulations. Note that only uniform and normal distributions were considered, as the uncertainty ranges sampled during the LHS UQ studies were either uniform or normal, indicating that the resulting distributions of predictions would follow a similar trend.

As evident by the plot shown in figure 6, the predictions of the split ring's gap width are better fit to a normal distribution. Thus, a residual stress prediction can be delivered, which accounts for the uncertainty associated with the model's sensitive parameters. Particularly, since the split ring corresponds best to the normal distribution, predictions of its gap width can be reported as a mean value plus-or-minus the standard deviation, or 28.5 mm ± 1.4%.

Lastly, as a final comparison of these representative predictions with the experimental data shown in figure 2, the simulated 100 residual stress responses were used to generate uncertainty bands. Specifically, figure 7 show uncertainty bands representative of the plausible regions, or distributions, in which realistic predictions of the cylinder's change in gap width will fall.

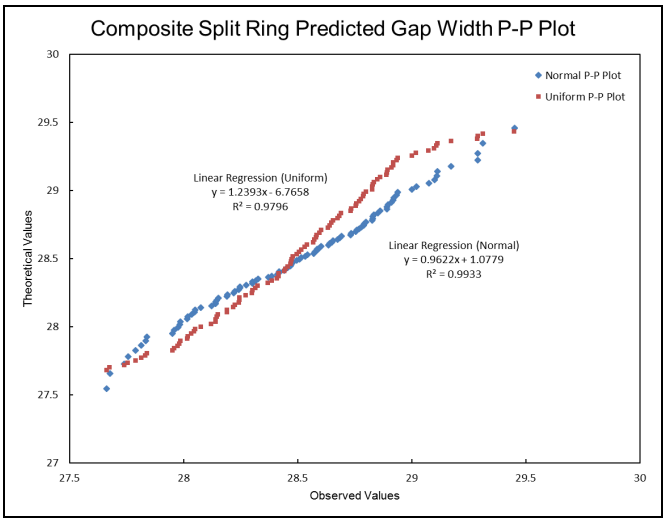

Figure 6: P-P plots for the composite split ring

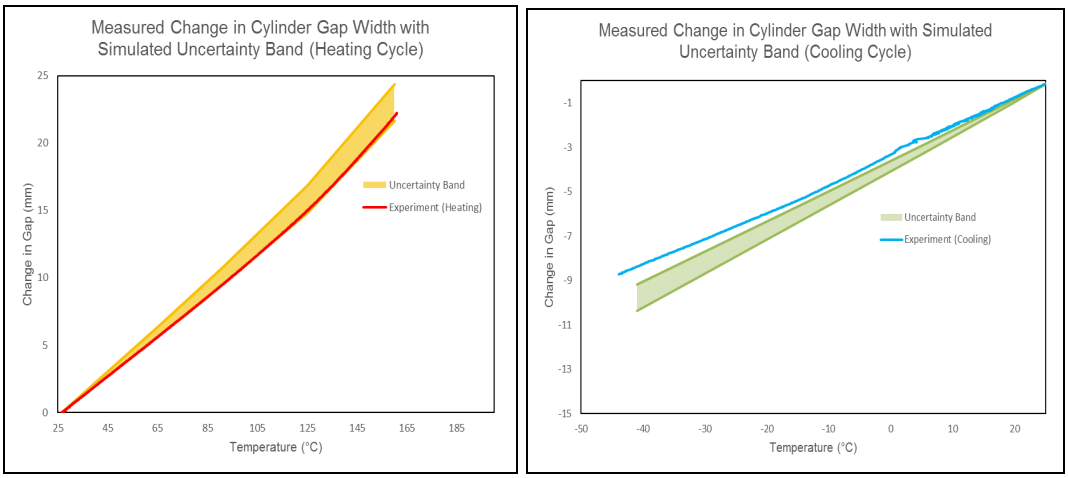

Figure 7: Experimental data and predicated distribution of the split ring's change in gap width

As shown in figure 7, the uncertainty bands provide reasonable agreement with the experimental data, indicating that it is more accurate to represent predictions of the residual stress state as a distribution, instead of a single value, as there are variations in the material property data that must be accounted for in the reported solutions. However, the simulated uncertainty bands do not completely encapsulate the recorded experimental data. It is possible that the inclusion of temperature dependence within the simulated materials could improve the agreement. Depending upon the orientation of the composite's reinforcing fibers, the elastic properties will soften as the temperature is increased and stiffen as the test temperature is decreased. According to these general trends, the agreement between the model predictions and experimental measurements would be improved. Since, at higher temperatures the elastic properties would decrease, leading to a decrease in the residual stresses and, alternatively, at lower temperatures, the elastic properties would increase along with the residual stresses.

4. CONCLUSIONS

The design of composite structures requires consideration of such material specific phenomena as process-induced residual stresses. Therefore, a simple and robust modeling methodology was developed that is capable of predicting a composite structure's post-fabrication residual stress state. With this method, which is based upon modeling approaches found in literature, the process-induced stresses are formed due to differences in the composite materials' coefficients of thermal expansion and thermal excursions from an experimentally determined stress-free temperature. Concurrent with the model development, experiments were designed and completed to quantify the residual stresses formed in a simple composite part. Specifically, a composite split ring was designed and manufactured such that measurable residual stresses were present. Upon completion of the residual stress experiment, the developed modeling methods were applied to approximate the manufacturing process of the composite ring for validation. However, because uncertainty was known to exist in several of the model's input parameters, formal sensitivity and uncertainty quantification studies were completed in the process of validating the modeling methods. Upon completion of these verification and

validation activities, the simulated residual stress predictions were found to be within an accurate range of the measurements recorded during the physical experiment. This indicates that it may be more accurate to represent the residual stress predictions as distributions, instead of as single values, as there are variations and unknowns in the material property data that must be accounted for in the reported solutions.

5. REFERENCES

1. Yokozeki, T., Ogasawara, T., Aoki, T. "Correction Method for Evaluation of interfacial fracture toughness of DCB, ENF and MMB Specimens with Residual Thermal Stresses." *Composites Science and Technology* 68 (2008): 760-767.
2. Nairn, J. "Energy Release Rate Analysis for Adhesive and Laminate Double Cantilever Beam Specimens Emphasizing the Effect of Residual Stresses." *International Journal of Adhesion and Adhesives* 20 (2000): 59-70.
3. White, S.R., Hahn, H.T. "Process Modeling of Composite Materials: Residual Stress Development during Cure. Part I. Model Formulation." *Journal of Composite Materials* 26 (1992): 2402-2422.
4. White, S.R., Hahn, H.T. "Process Modeling of Composite Materials: Residual Stress Development during Cure. Part II. Experimental Validation." *Journal of Composite Materials* 26 (1992): 2423-2453.
5. Tavakol, B., Roozbehjavan, R., Ahmed, A., Das, R., Joven, R.m Koushyar, H., Rodriguez, A., Minaie, B. "Prediction of Residual Stresses and Distortion in Carbon Fiber-Epoxy Composite Parts Due to Curing Process Using Finite Element Analysis." *Journal of Applied Polymer Science* (2013): 941-950.
6. Jumbo, F.S., Ashcroft, I.A., Crocombe, A.D., and Abdel Wahab, M.M. "Thermal residual stress analysis of epoxy bi-material laminates and bonded joints." *International Journal of Adhesion & Adhesives* 30(2010):523-538.
7. Hanson, A., Nelson, S., Briggs, T., Werner, B., Volk, B., Storage, T. "Experimental Measurement and Finite Element Analysis of Residual Stresses in Simple Composite Structures." *CAMX 2016*, Anaheim, CA, 2016.
8. SIERRA SolidMechanics Team (2015). *SIERRA/SolidMechanics 4.38 User's Guide*, Sandia National Laboratories, Albuquerque, NM.
9. Metals Handbook, Vol.2 - Properties and Selection: Nonferrous Alloys and Special-Purpose Materials, ASM International 10th Ed. 1990.
10. Roache, P. "Perspective: A Method for Uniform Reporting of Grid Refinement Studies." *Journal of Fluids Engineering* 116 (1994): 405-413.
11. Roache, P. "Verification of Codes and Calculations." *AIAA Journal* 36 (1998): 696-702.
12. Ferreira. S., Bruns, R., Ferreira, H., Matos, G., David, J., Brandao, G., da Silva, E., Portigal, L., dos Reis, P., Souza, A., and dos Santos, W. "Box-Behnken Design: An Alternative for the Optimization of Analytical Methods." *Analytica Chimica ACTA* 597 (2007): 179-186.
13. NIST/SEMATECH. (2013). *Engineering Statistics Handbook* [Online]. Available www.itl.nist.gov/div898/handbook
14. Niccoli, W., Marinelli, F., Fairbanks, T., and Dancause, R. "Latin Hypercube Sampling: Application to Pit Lake Hydrologic Modeling Study." *Conference on Hazardous Waste Research*, Montreal, Canada, 1998, Snowbird, Utah.
15. Sandia National Laboratories Dakota Team (2010). *Dakota, A Multilevel Parallel Object-Oriented Framework for Design Optimization, Parameter Estimation, Uncertainty Quantification, and Sensitivity Analysis Version 5.4 User's Manual*, Sandia National Laboratories, Albuquerque, NM.